THE JOURNAL OF PHYSICAL CHEMISTRY B

Article

pubs.acs.org/JPCB

Modeling of Fluorescence Quenching by Lutein in the Plant Light-Harvesting Complex LHCII

C. D. P. Duffy,*[,†] J. Chmeliov,[‡,§] M. Macernis,[‡,§] J. Sulskus,[‡] L. Valkunas,[‡,§] and A. V. Ruban[†]

[†]The School of Biological and Chemical Sciences, Queen Mary, University of London, Mile End Road, London E1 4NS, U.K.

[‡]Theoretical Physics Department, Faculty of Physics, Vilnius University, Saulėteko al. 9, LT-10222 Vilnius, Lithuania

[§]Institute of Physics, Center for Physical Sciences and Technology, Gostauto 11, LT-01108 Vilnius, Lithuania

Supporting Information

ABSTRACT: Photoprotective non-photochemical quenching (NPQ) in higher plants is the result of the formation of energy quenching traps in the light-harvesting antenna of photosystem II (PSII). It has been proposed that this quenching trap is a lutein molecule closely associated with the chlorophyll terminal emitter of the major light-harvesting complex LHCII. We have used a combination of time-dependent density functional theory (TD-DFT) and the semiempirical MNDO-CAS-CI method to model the chlorophyll−lutein energy transfer dynamics of the highly quenched crystal structure of LHCII. Our calculations reveal that the incoherent "hopping" of energy from Chl*a*612 to the short-lived, dipole forbidden $2^1A_g^-$ state of lutein620 accounts for the strong fluorescence quenching observed in these crystals. This adds weight to the argument that the same dissipative pathway is responsible for *in vivo* NPQ.

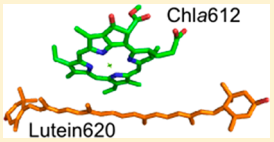

INTRODUCTION

Throughout natural history, one of the main challenges faced by photosynthetic organisms was living and evolving at very low levels of illumination, arising from life in aquatic environments, shading by competing organisms and other objects, cloud cover, etc. This selection pressure gave rise to the evolution of a light-harvesting antenna that is built of a number of pigment−protein complexes that serve to vastly enhance the spatial and spectral cross section of the reaction centers (RCs), the small, specific subset of chlorophylls responsible for photochemical charge separation. This arrangement ensures an optimal rate of energy delivery to the RCs despite low levels of illumination. However, as light exposure increases, particularly for the photosynthetic organisms that occupy land, this highly efficient *antenna* system can have a negative impact on the organism. The dangers posed by intense illumination arise from the fact that the maximum turnover rate of the RC is far slower than the rate of photon absorption and subsequent energy transfer in the antenna. Increasing illumination leads to a progressive saturation of the RCs. As more and more RCs are *closed*, there is a build-up of excitation energy within the antenna, leading to damage to photosystem II (PSII) which is particularly intense in the presence of oxygen. This damage, known as *photoinhibition*,[1] can take hours to reverse[2] and is seriously detrimental to the photosynthetic viability of the organism. However, evolutionary development has endowed some photosynthetic organisms, higher plants in particular, with the ability to cope with intense illumination through the collective action of many adaptive mechanisms. These mechanisms can deal with changes in light over a broad range of time scales, ranging from seasonal shifts to minute-by-minute fluctuations due to rapid changes in shading and cloud cover. For the most rapid fluctuations in light, this adaptation is made possible by the regulation of energy transduction in PSII by an enhancement of the nonradiative dissipation rate constant within the antenna. This regulation manifests itself as a decline in chlorophyll fluorescence yield of PSII in response to elevated illumination, a phenomenon known as non-photochemical quenching (NPQ).[3−7] The kinetics of NPQ formation and fluorescence recovery reveals several distinct components. The major component of NPQ is energy-dependent quenching (qE). qE normally forms in minutes in response to a rapid increase in illumination and relaxes equally quickly when light levels return to "normal". It is the qE component of NPQ that represents the rapid photoprotective adaptation of the organism. Some slower components of NPQ also reflect photoprotective energy dissipation and could be due to the formation of zeaxanthin (qZ) and entrapment of protons within the quenched antenna.[8] The mentioned fast (qE) and slow photoprotective components of NPQ are frequently referred to as "photoprotective NPQ". Another part of slowly reversible NPQ is attributed to the onset of photodamage−photoinhibitory quenching (qI). The qI component results from damage to a fraction of the RCs in PSII and can persist for several hours after the cessation of illumination. Essentially photoprotective NPQ arises from the formation of exciton-quenching trap sites within the antenna of PSII in high light.[9] These exciton-quenching sites capture excess excitation energy and dissipate it through some nonradiative process(es), thereby safely removing excess excitation energy from the antenna and reducing the excitation pressure felt by the RC. The phenomenon of photoprotective NPQ (pNPQ) and partic-

Special Issue: Rienk van Grondelle Festschrift

Received: July 24, 2012
Revised: December 11, 2012
Published: December 11, 2012

ularly its fast component, qE, has been the subject of intense study for over 40 years, and many of its features have been characterized extensively. For a detailed discussion of the topic, the reader is directed toward the recent review by Ruban and co-workers.[8] However, a brief discussion of some of its features and the current open questions within the field will follow.

It is known that "natural", *in vivo* pNPQ is driven by the interplay of three factors: A strong trans-membrane ΔpH, resulting ultimately from a high rate of photosynthetic charge separation;[10−13] the enzymatic de-epoxidation of the xanthophyll violaxanthin to zeaxanthin in the PSII antenna, the so-called *xanthophyll cycle*;[14−16] and the presence of the PsbS protein within the photosynthetic membrane.[17−19] It has been proposed that the collective action of these three mechanisms induces a subtle, reversible conformational change in the antenna pigment−protein complexes, thereby altering the landscape of interpigment interactions and leading to the formation of exciton quenching states.[20−26] However, despite extensive research, there is still no consensus concerning the exact molecular nature of the quenching sites, their precise location within the PSII antenna, and the exact physical mechanism(s) by which they are activated. It has been proposed that the transition to the dissipative state arises from the aggregation of LHCII in the photosynthetic membrane. This hypothesis was based on the fact that the *in vitro* aggregation of solubilized LHCII trimers (induced by the removal of detergent) results in significant fluorescence quenching.[27,28] This is further supported by the fact that crystal aggregates of LHCII (from which the atomistic structure was obtained[29,30]) are also quenched.

With regard to the nature and location of the quenching sites, there is a broad range of proposed models. The association between pNPQ and the xanthophyll cycle leads to the proposal of the *molecular gearshift model* of Frank and co-workers.[31] In this model, the dipole-forbidden, first singlet excited state (S_1) of violaxanthin lies above the S_1 state of chlorophyll *a*. In this scenario, there is absorption of light energy by the dipole-allowed S_2 state of violaxanthin, followed by rapid interconversion to the S_1 state and subsequent "downhill" energy transfer to chlorophyll. Violaxanthin therefore fulfills a light-harvesting role. However, the S_1 state of zeaxanthin was predicted to lie below the chlorophyll S_1 and so the direction of downhill energy flow is chlorophyll → zeaxanthin. Since the xanthophyll S_1 state is dipole forbidden, the only possible de-excitation pathway is interconversion (nonradiative dissipation) to the ground state. Typically, the S_1 state of a xanthophyll has a very short lifetime ($\tau \sim 10$ ps), making it an attractive candidate for the pNPQ quenching site(s).[32]

Another mechanism was proposed by Holt and co-workers who suggest that the formation of a chlorophyll−zeaxanthin charge transfer (CT) is responsible for excitation trapping with quenching proceeding via nonradiative charge recombination.[33] Initially, the location of this CT state was thought to be within LHCII, although the minor antenna was not excluded. However, recently Ahn and co-workers have proposed that this chlorophyll−zeaxanthin CT state resides in the minor antenna.[34] This model is somewhat undermined by the fact that quenching has been extensively observed in the absence of zeaxanthin[12,35] and, in the case of the model of Ahn and co-workers, by evidence that violaxanthin in the minor antenna is too strongly bound to the protein to be available for de-epoxidation.[36,37] However, if not zeaxanthin, there is significant evidence that pNPQ directly involves a xanthophyll of some type. Recently, Walla and co-workers suggested that qE is associated with an excitonic coupling between a chlorophyll S_1 state and a xanthophyll S_1 state.[38−41] Importantly, this was observed in the absence of zeaxanthin.[38] The transient absorption (TA) work of Ruban et al. on LHCII aggregates also showed that the qE component of pNPQ is associated with chlorophyll−xanthophyll interactions.[42] However, unlike the work of Walla and co-workers, these interactions were incoherent rather than excitonic, with energy being transferred from chlorophyll to the S_1 state of a xanthophyll, specifically lutein 1 in LHCII. This lutein is labeled lutein620 in the structure of Liu et al.[29] Lutein620 is an attractive candidate for the essential component in the qE mechanism. The inherently short lifetime of the xanthophyll S_1 state potentially makes it an effective *inherent quencher*. More importantly, its location within the LHCII structure shows it is in close contact with the *chlorophyll terminal emitter,* a closely associated aggregate of three chlorophyll *a* molecules (labeled Chl*a*610, Chl*a*611, and Chl*a*612 according to Liu et al.[29]) that represent the low energy "bottleneck" through which energy leaves LHCII on journey to the RC. A strong association with this chlorophyll energy sink is arguably a requirement of an effective quencher. However, Müller et al. performed identical TA measurements but found no evidence of xanthophyll involvement in quenching.[43] It is, however, worth noting that the TA traces of Ruban et al.[42] and Müller et al.[43] in the chlorophyll spectral regions are nearly identical, implying that differences in the modeling approaches used account for the different interpretations of the same data. Müller et al. have suggested that the quenching species is a low-lying chlorophyll−chlorophyll CT state.

In this paper, we outline a simple theoretical model of energy transfer within an isolated LHCII trimer, the geometry of which is taken from the high resolution crystal structure of Liu et al.[29] Specifically, we focus on the potential role of lutein620 as a site for energy quenching. Pascal et al. proposed that the crystal structure represents a highly quenched state based on the observation that crystallized LHCII has an average excited state lifetime of ∼0.89 ns compared to the ∼4 ns lifetime of isolated trimers.[44] An alternative viewpoint was presented by Barros et al.,[45] who contend that LHCII does not undergo any conformational change during pNPQ and therefore the crystal structure represents an unquenched, energy-collecting conformation. The decreased lifetime, and therefore the actual pNPQ mechanism, is attributed to interactions between trimers within crystals or aggregates. However, this conclusion is undermined by several experimental results. In 2008, Ilioaia and co-workers observed quenching in the complete absence of aggregation (LHCII immobilization in gel), indicating that intertrimer interactions are not essential to the pNPQ process.[46] This is further supported by the single molecule spectroscopy work of Krüger et al.[24,25,47] and theoretical model by Valkunas et al.[26] which showed that spatially isolated LHCII trimers can switch between a fluorescent and a quenched configuration. Additionally, resonance Raman spectroscopy has revealed that quenching is associated with a "twisting" in the configuration of the neoxanthin,[4248] and a significant change in the conformation of one of the luteins (labeled lut620 by Liu et al.) bound to LHCII.[49] Perhaps most relevant to our work, in 1998, Barzda et al. showed, using time-resolved laser flash photolysis, that aggregation-induced quenching is associated with a change in chlorophyll−xanthophyll interactions.[50] This was later confirmed by the flash-induced triplet-minus-singlet

(TmS_{flash}) and absorbance-detected magnetic resonance (TmS_{ADMR}) spectroscopy work of Lampoura et al.[51] It is possible that the quenching mechanism present within the crystal is closely related to the photoprotective quenching mechanism *in vivo*. Therefore, by modeling energy quenching within the LHCII crystal, we increase our understanding of *in vivo* qE. There have been several, highly accurate models of the energy transfer dynamics and optical properties of LHCII. The modified Redfield approach of Novoderezhkin et al. allowed for a simultaneous quantitative fit of the absorption, linear dichroism, and steady state spectra as well as the transient absorption kinetics.[52] Recently, Müh and co-workers produced a highly accurate *ab initio* model in which the effects of the protein/membrane/water environment were taken into account.[53,54] These studies illustrate the efficient nature of energy transfer within LHCII (and the antenna generally), with absorbed energy being transferred to the chlorophyll terminal emitter domain within a time scale of a few picoseconds. However, no such model has thus far explicitly included the role of the LHCII xanthophylls, due to the difficulty inherent in modeling the strongly correlated S_1 excited state.[55]

The molecular structure of the xanthophylls is based on the linear polyenes, extended, π-conjugated hydrocarbon chains. The S_1 state of these structures is usually labeled $2^1A_g^-$ according to its spatial symmetry. This state has the same symmetry as the ground state (S_0, or $1^1A_g^-$), and therefore an electric dipole transition between these two states is forbidden. The second singlet excited state (S_2 or $1^1B_u^+$) possesses different symmetries to the S_0 state and so is dipole allowed. Along with differences in symmetry, the S_1 and S_2 states differ in the relative importance of dynamic electron correlations, with the S_1 state being much more strongly correlated than S_2.[56] The fact that the S_1 state is so strongly correlated is the reason that it has proven difficult to model theoretically. Commonly used excited state methods such as the linear response formulation of time-dependent density functional theory (TD-DFT)[57,58] describe excited states as single-electron excitations. Inherent in such a single electron approach is the assumption that the excited states are weakly correlated. As such, *single excitation methods* like TD-DFT are inadequate for modeling the S_1 state of linear polyene systems such as xanthophylls.[56] Indeed, it has been shown that both single and *double* electron excitations must be considered to correctly model the strongly correlated S_1 state of carotenoids.[55,59] The difficulty in modeling the xanthophyll S_1 state, coupled with the fact that it is dipole forbidden and therefore cannot be directly probed by linear absorption/fluorescence experiments, means that there is some uncertainty regarding its excitation energy. Measurements of the S_1 energies of the LHCII xanthophylls have been made via excited state spectroscopy and transient absorption measurements.[32,60] It was found that the S_1 energy, ~13 900 cm^{-1} (1.73 eV or 719 nm), was the same for all three xanthophylls (lutein, violaxanthin, and neoxanthin). However, both of these methods are likely to probe the *relaxed* S_1 state rather than the vertical transition, and one would expect the vertical energy to be somewhat higher. In fact, Walla and co-workers directly measured the two-photon absorption spectrum of lutein in solution and found the S_1 peak (the vertical transition) at ~14 350 cm^{-1} (1.78 eV or 697 nm).[61] Unlike transient and excited state absorption, this technique probes the vertical transition. This value therefore gives us a reliable estimate of the lutein620 S_1 energy, although the *in situ* value will be determined by the solvatochromic effect of the protein environment.

The theoretical model presented here is novel in this respect. In this work, we explicitly include lutein620 in our calculations, with the goal of testing the physical feasibility of the quenching model based on the assumption that this xanthophyll is responsible for the qE quenching due to its interaction with the chlorophyll terminal emitter domain.[40]

METHODOLOGY

Geometry Optimization and Excited State Calculations. In order to study the possible role of lutein as a site for photoprotective energy quenching in LHCII, we must develop a theoretical description of the coupling between the S_1 states of chlorophyll and lutein. This first requires an accurate description of the excited states of both molecules. The starting point is the crystal structure of the isolated LHCII trimer as obtained by Liu et al.[29] In this model, we include all 42 chlorophylls and the three lutein620 molecules (one present per monomer). We shall neglect the other xanthophylls (lutein621, violaxanthin, and neoxanthin), which we argue is reasonable since the primary aim of this work is to test the proposed lutein620 quenching mechanism. Additionally, lutein620 is the only xanthophyll associated with the chlorophyll terminal emitter (see Figure 1). Since any absorbed

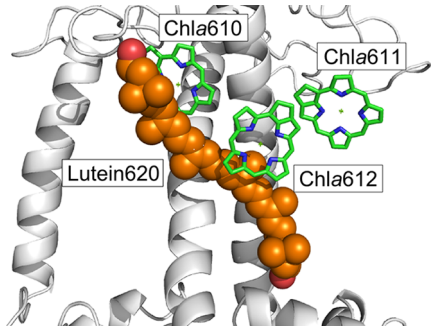

Figure 1. Lutein620 (gray spheres) is closely associated with the chlorophyll terminal emitter, three chlorophylls (black) that represent the energetic *bottleneck* through which energy leaves LHCII. The secondary structure of the protein scaffold is shown in white.

energy is rapidly transferred to the terminal emitter, we assume that chlorophyll → lutein620 transfer is the dominant chlorophyll → xanthophyll channel. The first step was to remove the phytol tails from the chlorophylls and replace them with a methyl group.[53,54] This vastly reduces the cost of subsequent calculations and has no significant effect on the low-lying singlet excited states that originate from electronic transitions between π-orbitals delocalized across the conjugated macrocycle of the chlorophyll "head" (see Figure 1). The next step is to add the hydrogen atoms missing from the crystal structure and then optimize the geometry of each pigment molecule individually. The resolution of the crystal structure, while sufficient to describe the bulk geometry of the pigment–protein complex, is insufficient to accurately describe quantum mechanically important parameters such as bond lengths, bond angles, and dihedrals. The structures must therefore be thoroughly reoptimized.[62] The geometry optimizations were performed using density functional theory (DFT)[63,64] with the CAM-B3LYP long-distance corrected exchange-correlation functional[65] and the 6-31G* Pople basis set,[66] as implemented

dx.doi.org/10.1021/jp3110997 | J. Phys. Chem. B 2013, 117, 10974–10986

in the Gaussian 09 quantum chemistry package.[67] This method was chosen, since it yields physically realistic geometries despite being computationally "cheap". However, to ensure that the overall structures of the individual pigments, i.e., the nonplanar distortions caused by interactions with the protein, the optimization is constrained. The constraints used were a freezing of certain dihedral angles. In the case of lutein620, all dihedrals along the conjugated backbone were constrained. A similar procedure was used for the chlorophylls in which all dihedrals along the outer ring of the conjugated macrocycle were frozen. The optimized structures were then mapped back onto the crystal structure such that the average deviation of the heavy atoms was minimized.

Calculation of the excitation energies and transition dipole moments of the S_1 transitions of chlorophylls were performed using TD-DFT within the Tamm−Dancoff approximation (TD-DFT/TDA)[68] as implemented by the ORCA quantum chemistry package.[69] The single excitation character of the excited states calculated by TD-DFT/TDA is sufficient for describing the weakly correlated chlorophyll singlet excited states. Both the S_1 and S_2 (for comparative purposes) states of lutein were calculated via a full configuration interaction (CI) calculation[70] on a complete active space (CAS) of molecular orbitals generated by the semiempirical modified neglect of differential overlap (MNDO) method[71] (MNDO-CAS-CI) as implemented by the MOPAC2006 semiempirical quantum chemistry package.[72] The MNDO-CAS-CI calculations were performed as part of a previous paper in which the application of this method to lutein (and its validity) is discussed extensively.[55] In this work, the dihedral distortions present in the lutein620 structure were modeled using the B3LYP hybrid functional[73] with the large 6-311++G(2d,p) Pople-style basis set. During these calculations, an unconstrained geometry optimization was performed and then dihedral distortions were added after the fact. The molecular properties calculated from these wave functions were then mapped onto lutein620 in our CAM-B3LYP structure of LHCII. It must be noted that, for the level of accuracy used here, these two structures are essentially equivalent. Indeed, the characters and CI compositions of the excited states (especially for $2^1A_g^-$) were not significantly affected by such dihedral distortions.[55] CI calculations based on the MNDO method have been successfully used to model the low-lying singlet excited states of carotenoids[59] as the full CI calculation allows for modeling of states with a multiply excited character (the xanthophyll S1 state is predominantly two-electron excitation[56]). As shall be discussed below, this study found that the best agreement between theory and experiment (in terms of the energy, symmetry, and CI character of the S_1 and S_2 states) was obtained with an active space consisting of six orbitals (three occupied and three virtual π-orbitals).

Transition Dipole Moments and Intermolecular Transfer Integrals. Below we shall outline a method for computing the transition dipole moments in terms of *atomic transition density moments*, T_α. Knowledge of the T_α then allows for computation of the chlorophyll−chlorophyll and chlorophyll−lutein *transfer integrals*, J_{DA}, in terms of pairwise interactions between atomic transition density moments.

The transition dipole moment for a transition between an excited state, $|EX\rangle$, and the ground state, $|GS\rangle$, of a molecule, M, is defined

$$\begin{aligned}\vec{\mu}_M &= \langle GS|\hat{\vec{\mu}}|EX\rangle \\ &= \sum_{i\in M} e\vec{r}_i\langle GS|\hat{N}_i|EX\rangle \\ &= \sum_{i\in M} e\vec{r}_i T_i,\end{aligned} \tag{1}$$

where i labels an *atomic orbital*, $\vec{r}_i$ is the central coordinate of the ith atomic orbital, and T_i is the transition density moment associated with the ith atomic orbital. The *number operator*, $\hat{N}_i$, is expressed in terms of *atomic orbital creation and annihilation operators*

$$\hat{N}_i = \sum_\sigma \hat{c}_{i\sigma}^\dagger \hat{c}_{i\sigma} \tag{2}$$

where $\hat{c}_{i\sigma}^{(\dagger)}$ annihilates (creates) an electron of spin σ in the ith atomic orbital. For notational convenience, we shall henceforth drop the circumflexes that denote operators. The atomic orbitals can be expanded in terms of *molecular orbital creation and annihilation operators*

$$\hat{N}_i = \sum_{\substack{m,m'\\ \sigma}} \beta_{im}^* \beta_{im'} a_{m\sigma}^\dagger a_{m'\sigma} \tag{3}$$

where $a_{m\sigma}^{(\dagger)}$ annihilates (creates) an electron of spin σ in the mth molecular orbital and $\{\beta_{im}\}$ are the *atomic orbital coefficients*. The total transition density moment associated with atom α is the sum

$$T_\alpha = \sum_{i\in\alpha} \langle GS|\hat{N}_i|EX\rangle \tag{4}$$

and so the transition dipole moment is given by

$$\vec{\mu}_M = \sum_{\alpha\in M} e\vec{r}_\alpha T_\alpha \tag{5}$$

where $\vec{r}_a$ is the central coordinate of the αth atom in molecule M.

$\{T_i\}$ can be computed from the wave functions generated by the TD-DFT/TDA and MNDO-CAS-CI calculations. For the TD-DFT/TDA calculations of the chlorophyll singlet excited states

$$|GS\rangle = |\psi_0\rangle \tag{6}$$

where $|\psi_0\rangle$ is the uncorrelated *reference determinant* determined by the initial self-consistent field calculation. The excited states are defined as a linear superposition of singly excited determinants which, for spin-conserving excitations, are defined as

$$|EX\rangle = \sum_{\substack{a\in\text{occupied}\\ r\in\text{virtual}\\ \sigma}} C_{a_\sigma}^{r_\sigma} |\psi_{a_\sigma}^{r_\sigma}\rangle \tag{7}$$

where $|\psi_{a_\sigma}^{r_\sigma}\rangle$ is the determinant obtained when an electron of spin σ is promoted from the ath occupied (the reference determinant) molecular orbital to the rth virtual molecular orbital and $C_{a_\sigma}^{r_\sigma}$ are the *CI coefficients*. In terms of molecular orbital operators,

$$|EX\rangle = \sum_{\substack{a,r\\ \sigma}} C_{a_\sigma}^{r_\sigma} a_{r\sigma}^\dagger a_{a\sigma} |\psi_0\rangle \tag{8}$$

Combining eqs 3 and 8, it is possible to show that[74]

$$T_i = \sum_{\substack{a,r \\ \sigma}} C_{a_\sigma}^{r_\sigma} \beta_{im}^* \beta_{im} \tag{9}$$

where both the CI and molecular orbital coefficients are available in the output of the TD-DFT/TDA calculations.

Both the S_1 and S_2 transitions of lutein were computed using MNDO-CAS-CI. Although the S_2 transition is not featured in the subsequent energy transfer dynamics simulation, it was important to confirm that this method gave reasonable results. Calculation of the transition dipole moments (and density moments) is far more involved than it is for the chlorophyll transitions but follows the same logic. In the case of MNDO-CAS-CI, both the ground state and the excited states are represented as CI wave functions. For the lutein calculations, it was found that only singly and doubly excited determinants contributed significantly ($C^2 > 0.01$) to the S_0 ($1^1A_g^-$), S_1 ($2^1A_g^-$), and S_2 ($1^1B_u^+$) states. These singlet states can be defined by

$$|S_x\rangle \simeq C_0|\psi_0\rangle + \sum_{\substack{a,r \\ \sigma}} C_{a_\sigma}^{r_\sigma}|\psi_{a_\sigma}^{r_\sigma}\rangle + \sum_{\substack{a\le b, r\le s \\ \sigma,\sigma'}} C_{a_\sigma b_{\sigma'}}^{r_\sigma s_{\sigma'}}|\psi_{a_\sigma b_{\sigma'}}^{r_\sigma s_{\sigma'}}\rangle \tag{10}$$

where $|\psi_0\rangle$ is the reference determinant generated by the initial MNDO calculation, $|\psi_{a_\sigma}^{r_\sigma}\rangle$ is a singly excited determinant as defined in eqs 7 and 8, and $|\psi_{a_\sigma b_{\sigma'}}^{r_\sigma s_{\sigma'}}\rangle$ is a doubly excited determinant. The doubly excited determinants are expressed in terms of molecular orbital operators

$$|\psi_{a_\sigma b_{\sigma'}}^{r_\sigma s_{\sigma'}}\rangle = -\theta_{rs} a_{s\sigma'}^\dagger a_{r\sigma}^\dagger a_{b\sigma'} a_{a\sigma}|\psi_0\rangle \tag{11}$$

where

$$\theta_{rs} = \begin{cases} 1 & \text{for } r \le t \\ -1 & \text{otherwise} \end{cases} \tag{12}$$

and the minus sign results from the ordering of the creation and annihilation operators. Using eqs 10−12, it is possible to obtain analytical expressions for T_i in analogy to eq 9, although the expressions have a much more complex functional form. The reader is directed to the Supporting Information for the derivation of these expressions.[75] When computing transition density moments from the results of our quantum chemistry calculations, we neglected, for simplicity, any terms in the CI expansion whose coefficient was $C^2 < 0.01$. The energetic coupling between the electronic transitions of molecules D and A is determined by the *intermolecular transfer integral*[76]

$$W_{DA} = J_{DA} - K_{DA} \tag{13}$$

where W_{DA} can be divided into terms mediated by the direct Coulomb interaction, J_{DA}, and the exchange interaction, K_{DA}.[77,78] Since the exchange interaction results from the overlap of atomic orbitals, it decreases exponentially with increasing intermolecular separation. We will therefore neglect, within this paper, its contribution to W_{DA}. The intermolecular coupling is therefore assumed to arise from the Coulomb interactions between transition densities and is most generally defined as[76]

$$\begin{aligned} J_{DA} &= \sum_{\substack{i\in D \\ j\in A}} V_{ij}\langle \mathrm{EX}_A|\hat{N}_j|\mathrm{GS}_A\rangle\langle \mathrm{GS}_D|\hat{N}_i|\mathrm{EX}_D\rangle \\ &= \sum_{\substack{i\in D \\ j\in A}} V_{ij} T_i^D T_j^A \end{aligned} \tag{14}$$

where V_{ij} determines the scale of the interaction between transition densities. If the two molecules are sufficiently separated, then

$$V_{ij} \cong \frac{e^2}{4\pi\varepsilon\varepsilon_0|\vec{r}_i - \vec{r}_j|} \tag{15}$$

where $\vec{r}_i$ is the central coordinate of the ith atom and ε is the relative dielectric permittivity of the surrounding medium. If the separation of the molecules is much greater than the spatial extension of the molecules, eq 14 reduces to an interaction between two transition dipole moments. However, due to the crowded nature of the pigments within LHCII, we shall adopt the monopole form as described by eq 15. In this work, the formalism defined above is used to compute the chlorophyll−lutein620 couplings in LHCII.

The transition dipole moments as calculated with *in vacuo* TD-DFT/TDA are typically overestimates of the real values. To compensate for this, the T_α values were rescaled so that the average dipole strengths were equal to the vacuum-extrapolated values determined by Knox and Spring (21.0 D^2 for chlorophyll *a* and 14.7 D^2 for chlorophyll *b*).[53,54,79] Since there is no corresponding vacuum extrapolation data for the xanthophyll S_1 transition (since it is effectively zero in all solvents), no such rescaling could be applied for lutein.

The dielectric effect of the protein environment was accounted for with a simple continuum model in which the T_α are embedded in a uniform dielectric material with a relative optical permittivity of $\varepsilon = 2$.[53,54] The chlorophyll−chlorophyll couplings are also calculated via this method but only for comparative purposes to demonstrate that our approach is consistent with the much more accurate work of Müh et al.[53,54] For the calculation of the chlorophyll−chlorophyll dynamics, we shall use the couplings given in the Supporting Information of Müh et al. (2010).[53]

Energy Transfer Dynamics. The initial assumption was that the energy transfer within an isolated trimer was described as an incoherent *hopping* between individual pigments. Conventional (dipole−dipole) Förster theory[80] predicts that there is no transfer between the chlorophyll and lutein S_1 states, since the lutein S_1 state is dipole forbidden. However, due to the close proximity of pigment molecules in LHCII, transfer involving dipole-forbidden states can be rapid.[81] The exciton dynamics in LHCII trimers is described by the master equations

$$\frac{\mathrm{d}}{\mathrm{d}t}P_i(t) = -\sum_{j\neq i}\left(k_{ij}P_i(t) - k_{ji}P_j(t)\right) - k_F P_i(t) - k_{NR}P_i(t) \tag{16}$$

where P_i is the exciton occupation probability of the ith pigment (site), k_F and k_{NR} are the radiative (fluorescence) and nonradiative decay rates, respectively, and the interpigment transfer rates, k_{ij}, from the ith to the jth site are given by

$$k_{ij} = \frac{2\pi}{\hbar}|J_{ij}|^2 \int \mathrm{d}E f_i(E) f_j(E) \tag{17}$$

The integral represents a measure of the energetic overlap between donor i and acceptor j. As with our previous work,[74] we have assumed that the densities of states, $f(E)$, were normalized Gaussian functions

$$\int \mathrm{d}E f_i(E) f_j(E) \rightarrow \frac{1}{\sqrt{2\pi(\sigma_i^2 + \sigma_j^2)}} \exp\left\{\frac{-(E_i - E_j)^2}{2(\sigma_i^2 + \sigma_j^2)}\right\} \tag{18}$$

where $\sigma_{i(j)}$ is the standard deviation of the Gaussian line centered at $E_{i(j)}$ for molecule i (j). The widths of these density-of-state functions were found by Gaussian fitting of the relevant absorption spectra. For the chlorophylls, average standard deviations were taken from the multi-Gaussian fitting of the room temperature chlorophyll absorption spectrum of LHCII, as performed by Zucchelli et al.[82] This gave an average standard deviation of $\sigma \approx 12$ meV (97 cm^{-1}) for chlorophyll *a* and $\sigma \approx 15$ meV (121 cm^{-1}) for chlorophyll *b*. For the lutein S_1 transition, a single Gaussian function was fit to the two-photon absorption spectrum of Walla et al.[61] Despite the noise present in this data, a decent fit was obtained (mean relative square error $R^2 = 0.993$) which gave a large value of $\sigma \approx 152$ meV (1225 cm^{-1}), reflecting the very broad nature of the xanthophyll S_1 transition. The hopping rates are strongly determined by site energies of the chlorophylls. As such, we use the chlorophyll site energies determined by Novoderezhkin et al.[52] and the fitted values (model A) of Müh et al.[53] rather than the energies obtained from our *in vacuo* calculations. Since the actual energy of the *in situ* vertical energy of the lutein S_1 transition is uncertain, this is treated as a (moderately) free parameter. For calculating the excited state lifetime, kinetics, and fluorescence quantum yield, we require estimates of the rates of radiative and nonradiative decay of the S_1 states of the pigments. Chlorophyll in dilute solution has a fluorescence quantum yield of $\varphi_F \approx 0.3$ and an excited state (S_1) lifetime of $\tau_{total} \approx 5$ ns.[83] This gives an S_1 fluorescence rate of $k_F \approx 6.0 \times 10^7$ s^{-1} and a nonradiative rate of $k_{NR} \approx 1.4 \times 10^8$ s^{-1}. This nonradiative rate is a combination of slow ($\sim 2.0 \times 10^7$ s^{-1}) interconversion and the faster intersystem crossing ($\sim 1.8 \times 10^8$ s^{-1}). However, for the purposes of the model, a single, nonspecific, nonradiative decay channel is assumed. For the lutein S_1 state, $k_F = 0$, since it is dipole forbidden, and $k_{NR} \approx 1.0 \times 10^{11}$ s^{-1} due to the extremely short lifetime (~10 ps) of the state. Throughout this work, it is assumed that there is no geometric relaxation of the S_1 states of the pigments.

The initial condition for eq 16 was chosen to be a single exciton per whole LHCII trimer with equal probabilities to be localized over any of 42 chlorophylls:

$$P_i(0) = \begin{cases} 1/42 & \text{for chlorophylls} \\ 0 & \text{for luteins} \end{cases} \tag{19}$$

As the system evolves in time, the exciton population is lost through fluorescence and nonradiative decay (quenching). It is also assumed that the transfer rates k_{ij}, calculated according to eq 17, satisfy the requirements of *detailed balance*, where forward and backward hopping rates are rescaled: if $E_i > E_j$,

$$k_{ij} \equiv k$$
$$k_{ji} = k \exp\left(-\frac{\Delta E}{k_B T}\right) \tag{20}$$

The effects of excitation delocalization (coherence) on quenching by lutein were also tentatively studied. An approach often used is the *block diagonalization* method, in which excitonic effects are only taken into account for localized states with a coupling greater than some cutoff, J_c.[53,54,84,85] This cutoff energy is related to the energetic scale of the dynamic localization (dephasing) of the excitonic states. There is some uncertainty regarding the choice of cutoff. Müh et al. found that the linear absorption spectrum of LHCII was largely insensitive to this value. However, a value of $J_c \approx 2.5$ meV (20 cm^{-1}) was required to fit the CD spectrum.[53] However, a range of cutoff values (20−120 cm^{-1}) has been used in other studies of related pigment−protein complexes.[84,85] As will be shown below, we found that the fluorescence quenching of the model was independent of whether chlorophyll−chlorophyll coherence was or was not accounted for. Generally, if the calculated incoherent hopping time between two pigments was sub-ps, we supposed that the assumption of incoherent transfer was probably inadequate, and excitonic effects were investigated. Such chlorophyll pairs typically had a coupling strength in the 3−9 meV (20−70 cm^{-1}) range.

After determining for which chlorophyll pairs (or triples, in the case of the terminal emitter Chl*a*610−Chl*a*611−Chl*a*612) the excitonic effects should be treated, we augmented the coupling matrix **J** with the corresponding pigments' site energies on its diagonal and performed the unitary transformation, resulting in the block diagonalization for the excitonically coupled chlorophylls. As a result, excitonic energy levels and the couplings between them and solitary chlorophylls were obtained. The densities-of-states of these excitonic levels E_α (depending on the initial site energies E_i), used later to compute transfer rates, were assumed to be the normalized Gaussian functions with the standard deviation σ_α estimated according to standard rules for the combined variances as

$$\sigma_\alpha = \sqrt{\sum_{i=1}^{2\text{ or }3} \left(\frac{\partial E_\alpha}{\partial E_i} \cdot \sigma_i\right)^2}$$

where σ_i is the standard deviation of the density-of-states of the particular pigment in the dimer (or trimer). For a particular chlorophyll pair/triple, it was assumed that relaxation to the lowest energy excitonic state occurred essentially instantaneously, a reasonable assumption given the energetic proximity of these delocalized states. We must stress that this treatment of excitonic interactions is approximate. However, we are less interested in the precise details of the chlorophyll−chlorophyll dynamics than we are in the interactions between chlorophyll and lutein620. A more precise treatment of excitonic couplings between the chlorophylls in LHCII is the subject of much study and will represent a future refinement to our model.

In addition to the general treatment of excitonic delocalization, we also decided to investigate the validity of a particular model of qE quenching, supported by the work of Mozzo et al.,[41] that involves excitonic interactions between chlorophyll and lutein620 within LHCII. Van Amerongen and van Grondelle proposed[86] that a small amount of excitonic mixing between S_1 states of a xanthophyll and a chlorophyll results in a pseudochlorophyll S_1 state with a dramatically shortened excited state lifetime. The energetic splitting of the two single molecule states is given by

$$\epsilon_\pm = \frac{(E_{xanth} + E_{chl})}{2} \pm \frac{((E_{xanth} - E_{chl})^2 + 4|J|^2)^{1/2}}{2} \tag{21}$$

where E_{xanth} and E_{chl} are the energies of the original xanthophyll and chlorophyll S_1 transitions and $\epsilon_\pm$ are the energies of the

Table 1. The S_1 Transition Energies, Dipole Strengths, and Standard Deviations of the Density-of-States of the LHCII Chlorophylls and Lutein620[a]

	Transition Energies (eV)			Dipole Strengths (D^2)		
pigment	calculated (vacuum)	Novoderezhkin et al.	Müh et al. (fitted model A)	calculated (vacuum)	rescaled	σ (meV)
Chl*b*601	2.26	1.97	1.91	20.7	13.6	14.8
Chl*a*602	2.27	1.88	1.85	40.5	20.6	11.8
Chl*a*603	2.27	1.90	1.84	41.3	20.4	11.8
Chl*a*604	2.25	1.92	1.84	45.3	23.5	11.8
Chl*b*605	2.25	1.94	1.92	22.4	15.2	14.8
Chl*b*606	2.26	1.97	1.91	28.4	18.9	14.8
Chl*b*607	2.25	1.95	1.90	22.8	15.8	14.8
Chl*b*608	2.26	1.95	1.88	19.2	12.8	14.8
Chl*b*609	2.26	1.95	1.91	18.9	12.3	14.8
Chl*a*610	2.26	1.87	1.83	42.2	20.5	11.8
Chl*a*611	2.27	1.87	1.85	41.6	19.9	11.8
Chl*a*612	2.27	1.87	1.85	42.6	21.8	11.8
Chl*a*613	2.26	1.88	1.84	44.8	19.1	11.8
Chl*a*614	2.27	1.89	1.85	43.1	22.3	11.8
lutein620	2.49 (2.85)			0.0 (272.4)		151.8

[a]Also shown are the site energies proposed by Novoderezhkin et al.[52] and Muh et al.[53] and the rescaled transition dipole strengths. For lutein620, the S_2 energy and dipole strength are listed within brackets.

excitonic states arising from the interaction. Since $E_{xanth} < E_{chl}$, the excitonic states are given by

$$|+\rangle = \cos\left(\frac{\theta}{2}\right)|\mathrm{chl}\rangle + \sin\left(\frac{\theta}{2}\right)|\mathrm{xanth}\rangle \tag{22}$$

and

$$|-\rangle = -\sin\left(\frac{\theta}{2}\right)|\mathrm{chl}\rangle + \cos\left(\frac{\theta}{2}\right)|\mathrm{xanth}\rangle \tag{23}$$

where the mixing angle is defined by

$$\tan\theta = \frac{2J}{|E_{chl} - E_{xanth}|}, \quad 0 \le \theta < \pi \tag{24}$$

In this model, it is proposed that the coupling between the two transitions is weak ($J \ll |E_{chl} - E_{xanth}|$) and therefore it only slightly perturbs the original, uncoupled states. However, the pseudochlorophyll state now contains a small contribution from the xanthophyll state and vice versa. Assuming that the degree of mixing is only 2%,

$$|+\rangle = 0.99|\mathrm{chl}\rangle + 0.14|\mathrm{xanth}\rangle \tag{25}$$

and

$$|-\rangle = -0.14|\mathrm{chl}\rangle + 0.99|\mathrm{xanth}\rangle \tag{26}$$

we obtain that despite the small xanthophyll component the pseudochlorophyll state has a much shortened lifetime

$$\frac{1}{\tau_+} \approx 0.99^2\left(\frac{1}{5\ \mathrm{ns}}\right) + 0.14^2\left(\frac{1}{0.01\ \mathrm{ns}}\right) \approx \frac{1}{450\ \mathrm{ps}} \tag{27}$$

It is therefore possible that excitonic rather than incoherent chlorophyll−xanthophyll interactions are responsible for qE-related energy quenching.

RESULTS

Excited State Calculations. The S_1 states of the chlorophylls, as computed using TD-DFT/TDA, are predominantly a superposition of a single-electron HOMO → LUMO and a single-electron HOMO−1 → LUMO+1 transition. The site energies and transition dipole moments (as calculated via the transition density moment method outlined above) are listed in Table 1.

The electronic states of lutein620 are more complex. First, the ground state (S_0) is predominantly the reference determinant (C_0 = +0.9) but also contains significant contributions from the single-electron HOMO → LUMO+1 excitation ($C_{H_\uparrow}^{L_\uparrow} = C_{H_\downarrow}^{L_\downarrow} = -0.11$) and the double-electron HOMO → LUMO excitation ($C_{H_\uparrow H_\downarrow}^{L_\uparrow L_\downarrow} = -0.14$). This state is a singlet, has A_g^- symmetry, and so appears to be a realistic description of the $1^1A_g^-$ ground state. The first singlet excited state (S_1) also has A_g^- symmetry and has the double-electron HOMO → LUMO ($C_{H_\uparrow H_\downarrow}^{L_\uparrow L_\downarrow} = -0.58$) and the single-electron HOMO → LUMO+1 ($C_{H_\uparrow}^{L+1_\uparrow} = C_{H_\downarrow}^{L+1_\downarrow} = +0.25$) and HOMO−1 → LUMO ($C_{H-1_\uparrow}^{L_\uparrow} = C_{H-1_\downarrow}^{L_\downarrow} = -0.27$) transitions. This state is dipole-forbidden, having a dipole strength of 0.00 D^2 due to the fact it has the same symmetry as the ground state. This state appears to be a physically reasonable description of the lutein S_1 state. However, the excitation energy of this state is ∼2.5 eV (20 210 cm^{-1}), which is significantly higher than the two-photon peak of the lutein S_1 state in solution as measured by Walla et al.[61] The $1^1B_u^+$ state (the canonical S_2 state) has the single HOMO → LUMO excitation ($C_{H_\uparrow}^{L_\uparrow} = C_{H_\downarrow}^{L_\downarrow} = -0.52$) as its major component, with significant contributions from both singly and doubly excited determinants with B_u^+ symmetry. This state is strongly dipole-allowed with a dipole strength of ∼270 D^2. This corresponds to a dipole length of ∼16.5 D, which is in reasonable agreement with the reported dipole length of ∼15 D.[87,88] The calculated excitation energy is ∼2.85 eV (23040 cm^{-1}), which is an overestimate of the experimental value of 2.5−2.7 eV.[87,88] The CI compositions of these states are listed in detail in the Supporting Information,[75] and the reader is directed to our earlier paper for a full discussion of the MNDO-CAS-CI description of linear polyene and xanthophyll excited states.[55]

Chlorophyll−Chlorophyll and Chlorophyll−Lutein Couplings. The S_2 state of lutein was computed only as a measure of the reasonability of the chosen quantum chemical

dx.doi.org/10.1021/jp3110997 | J. Phys. Chem. B 2013, 117, 10974−10986

method. Since the proposed quenching mechanism being examined in this work involves only the S_1 transition, it is not used within the energy transfer model. The matrix of chlorophyll−chlorophyll and chlorophyll−lutein transfer integrals for the LHCII trimer, as calculated by eq 14, is listed in the Supporting Information. To account for the screening effect of the protein environment, we assumed that the transition monopoles were embedded within a continuous dielectric medium with a relative dielectric constant of $\varepsilon = 2$. We compared our chlorophyll−chlorophyll couplings to those obtained by Müh et al.[53] using a much more accurate method. Our results were in good agreement despite our simplistic treatment of the solvent environment and its effect on the transition densities. Importantly, the relative signs and magnitudes of the couplings were in good qualitative agreement. Within the LHCII monomer, we identified several strongly coupled chlorophyll pairs. These were also the most strongly associated chlorophyll pairs identified by Müh et al.[53] These are listed in Table 2. We note that lutein620 appears to be moderately coupled ($J \approx -1.7$ meV) to Chl*a*612 and only weakly coupled ($|J| \approx 0.1-0.2$ meV) to Chl*a*608 and Chl*a*610. It essentially has a negligible interaction with the other more distant chlorophylls.

Table 2. The Couplings between Strongly Associated Chlorophylls within the LHCII Monomer[a]

chlorophyll pair	J (meV)	J (meV) as calculated by Müh et al.
*a*611−*a*612	12.0	12.3
*a*603−*b*609	9.7	8.9
*a*604−*b*606	7.1	8.8
*b*601−*a*602	5.2	4.5
*b*608−*a*610	5.1	5.3

[a]We compare our values with those of Müh et al.[53]

Energy Transfer Dynamics. The matrix of *hopping times* ($1/k_{ij}$) for incoherent energy transfer between chlorophylls is included in the Supporting Information.[75] These values show the distinct energy transfer pathways within the trimer and illustrate the efficient nature with which energy is transferred to the terminal emitter domain within a few ps. In this model, we initially assume that each monomer in the isolated LHCII trimer contains an identical lutein quenching site; i.e., the site energy is the same in each monomer. In the absence of the chlorophyll → lutein pathway, the fluorescence quantum yield of the isolated trimer is, by our previous definition, $\varphi_F = 0.3$, corresponding to a completely unquenched chlorophyll system. When the lutein pathway is present, we observe a significant reduction in the excited state lifetime and fluorescence quantum yield indicating that this pathway represents a highly efficient fluorescence quencher. However, it was found that the degree of quenching was highly sensitive to the lutein S_1 energy. The net Chl*a*612 → lutein hopping rate as a function of lutein620 site energy is shown in Figure 2A. We observe a weak dependence for $E_{Lut} < E_{a612}$ followed by the obvious discontinuity and step increase as $E_{Lut} \geq E_{a612}$. The fastest hopping rate occurs at $E_{Lut} = 1.80-1.85$ eV. Importantly, we see that the hopping rate, even at this optimum energy, is slow with respect to both chlorophyll−chlorophyll transfer and the excited state lifetime of the lutein S_1 state.

φ_F is also, as expected, very sensitive to the lutein620 site energy, as shown in Figure 2B for the chlorophyll site energies reported by Novoderezhkin et al.[52] and Müh et al.[53] The maximum fluorescence quenching occurs at $E_{Lut} \approx 1.80$ meV for both sets of site energies, a value very close to the two-photon peak measured by Walla et al.[61] We also note that quenching is more efficient when using the chlorophyll site energies of Novoderezhkin et al.[52] However, both sets of site energies produce essentially the same results (in a qualitative sense) and so we shall hereafter focus our attention on the results obtained using the chlorophyll site energies of Müh et al.[53]

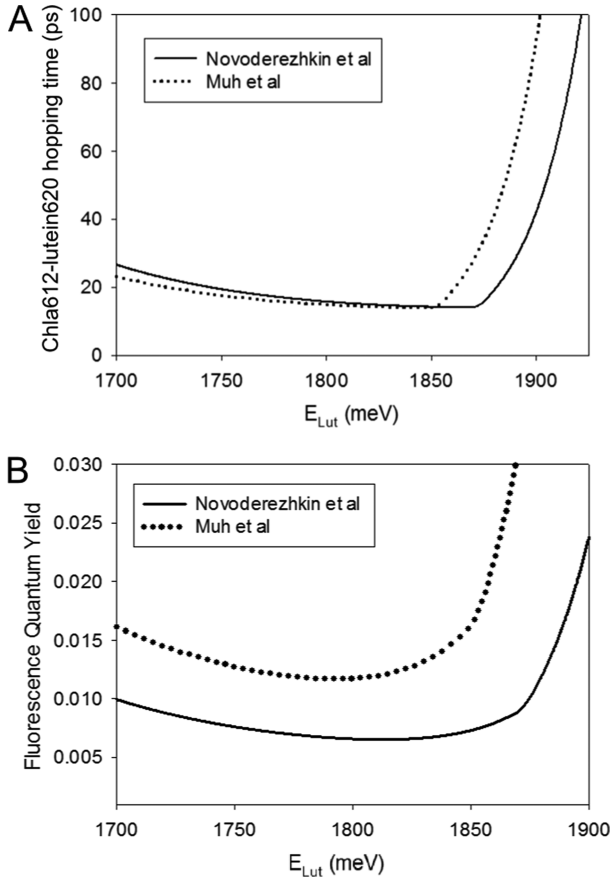

Figure 2. Part A shows the net Chla612 → lutein620 *hopping rate* as a function of E_{Lut} for the chlorophyll site energies reported by Novoderezhkin et al.[52] and Muh et al.[53] Part B shows the fluorescence quantum yield of an isolated LHCII trimer as a function of E_{Lut} for the chlorophyll site energies reported by Novoderezhkin et al.[52] and Muh et al.[53]

The excited state kinetics of the trimer, as a function of lutein620 site energy, are shown in Figure 3. This illustrates that decrease in fluorescence quenching as the energy increases above the optimum value of $E_{Lut} \approx 1.8$ eV. The kinetics also slow down as E_{Lut} drops below this level albeit not rapidly. Since the lifetime of the lutein S_1 state is so short, the kinetics are well described by a single exponential decay; i.e., the transfer of energy from lutein back into the chlorophyll bulk (detrapping) is negligible. The excited state lifetimes of the trimer are listed in Figure 3 and again show that the chlorophyll → lutein620 pathway results in very strong fluorescence quenching. However, we see that, in the $E_{Lut} \sim E_{a612}$ range, ∼1.85 eV (14 900 cm^{-1}), a blue shift of the lutein S_1 state of ∼25 meV (9 nm) results in an increase in the LHCII lifetime by a factor of 2.

Taking into account excitonic effects (in an approximate sense), we identified several "clusters" of chlorophylls that were

dx.doi.org/10.1021/jp3110997 | J. Phys. Chem. B 2013, 117, 10974−10986

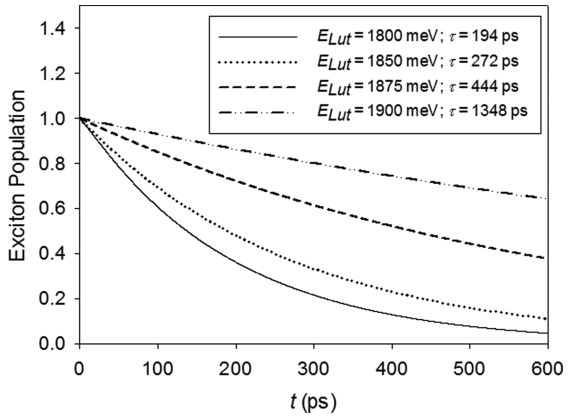

Figure 3. The excited state kinetics of an isolated LHCII trimer as a function of E_{Lut} for the chlorophyll site energies reported by Muh et al.[53] The mean excitation lifetimes, τ, of the corresponding kinetics are listed in the legend.

very strongly coupled, implying that excitonic delocalization should be accounted for. Most importantly, within each monomer, the terminal emitter domain, Chl*a*610−Chl*a*611−Chl*a*612, appears to form a single cluster resulting in three delocalized excitonic states. Chla613−Chla614 also forms an intramonomer cluster. This approach also implied excitonic delocalization between different LHCII monomers, with delocalization occurring between Chl*b*601 and Chl*a*609. We note at this point that, by the criteria outlined in the Methodology section, it is unlikely that there is any significant excitonic interaction between chlorophyll and the lutein620 S_1 state as a result of the small coupling between states. The new matrix of chlorophyll−chlorophyll couplings, J_{DA}, which includes couplings involving these delocalized states, is included in the Supporting Information.[75] The net hopping rates for transfer from the delocalized terminal emitter states to lutein620 are shown in Figure 4A. We see clearly that transfer between the upper two terminal emitter states and lutein620 is slow, even in the optimum case of $E_{Lut} \approx 1.8$ eV. Transfer from the lowest excitonic state is negligible. The fluorescence quantum yield of the LHCII trimer with excitonic delocalization is shown in Figure 4B. It is apparent that the approximate inclusion of excitation delocalization has no significant effect on fluorescence quenching by lutein620.

So far we have neglected excitonic interactions between lutein620 and the terminal emitter due to the small intermolecular coupling. However, as described above, weak lutein620−chlorophyll interactions have been proposed as a central feature of the qE quenching mechanism.[41,86] Figure 5 shows the lifetime of the pseudo chlorophyll state as a function of lutein620 S_1 excitation energy, as estimated by eq 26. We note that the assumption inherent in this approach is that the original uncoupled states remain good approximations of the resulting excitonic states. This is only valid in the limits $E_{Lut} \ll E_{Chla612}$ and $E_{Lut} \gg E_{Chla612}$. This simple calculation shows that for $E_{Lut} \sim 1.78$ eV excitonic delocalization lowers the lifetime of the pseudo-Chl*a*612 state to ∼3.5−4 ns. This is significantly longer than the sub-ps (∼650 ps) lifetime suggested in the excitonic model of qE quenching[38−41,86] and is insufficiently large to account for the quenching observed in the LHCII crystal structure. Of course, the lifetime of the pseudo-Chl*a*612 drops as the lutein620 and Chl*a*612 states become closer in energy. The lifetime of the pseudo-Chl*a*612 state drops below 1

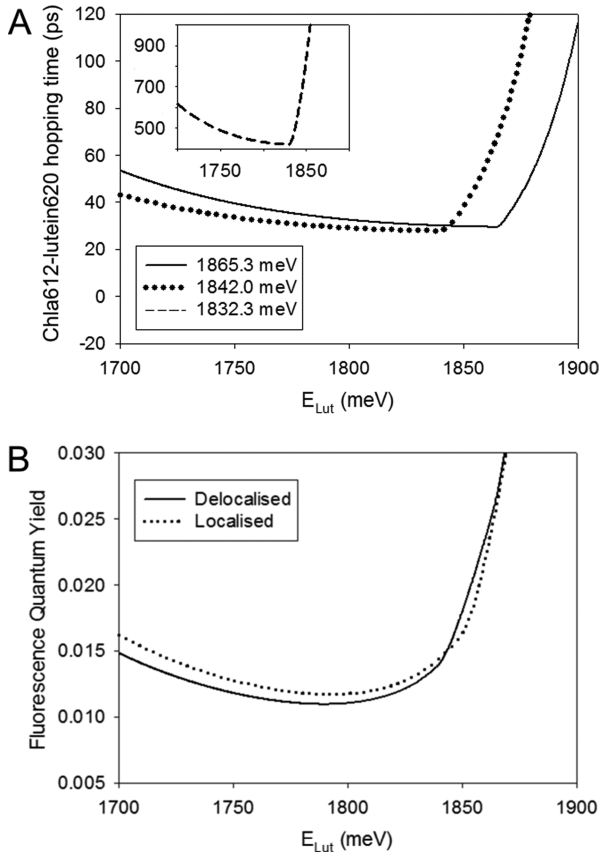

Figure 4. Part A shows the net hopping rate for energy transfer between the delocalized terminal emitter states and lutein620 as a function of E_{Lut} for the chlorophyll site energies reported by Müh et al.[53] The delocalized Chl*a*610−Chl*a*611−Chl*a*12 states are labeled in terms of their excitation energy. The slow rate for the negligible hopping between the lowest excitonic state and lutein620 is shown in the inset. Part B shows the fluorescence quantum yield of an isolated LHCII trimer as a function of E_{Lut} when excitonic delocalization is present. The data presented in Figure 2B (for localized states) is also displayed for comparison. The chlorophyll site energies are those reported by Müh et al.[53]

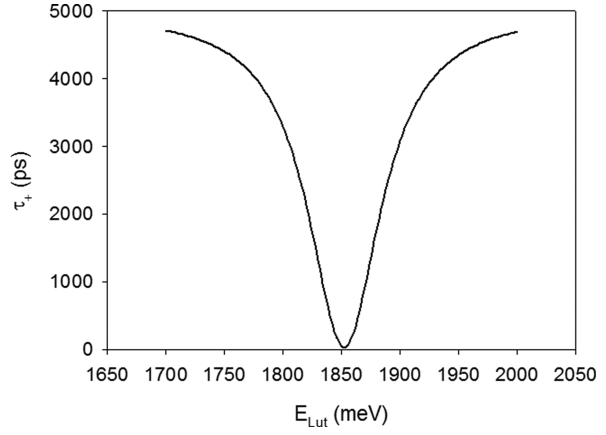

Figure 5. The lifetime of the excited state of the pseudo-Chl*a*612 excitonic state as estimated using eq 27. It should be noted that this approach is only valid in the limits $E_{Lut} \ll E_{Chla612}$ and $E_{Lut} \gg E_{Chla612}$.

ns when $E_{Chla612} - E_{Lut} \sim 0.01$. However, at this point, according to eqs 22 and 23, the excitonic states will be, to a very good approximation, equal mixtures of the uncoupled single

dx.doi.org/10.1021/jp3110997 | J. Phys. Chem. B 2013, 117, 10974−10986

molecule states ($\cos(\theta/2) \approx \sin(\theta/2) \approx 0.70$). The excitonic states are therefore completely delocalized across the two molecules and can no longer be said to resemble the original states. This would require a significant (~800 meV) blue shift of the lut620 S_1 state and also deviates from the model proposed by van Amerongen and van Grondelle.[86]

Trap Density. Lastly, we studied the effect of trap density on the fluorescence quantum yield of the trimer. Throughout we have assumed that each monomer contained an identical lutein620 trap. Of course, real systems such as the LHCII crystals or the *in vivo* PSII antenna will possess a degree of heterogeneity. Variation in the chlorophyll−lutein620 coupling and the relative site energies will mean that our assumption that each monomer is identical is unrealistic. In reality, it is likely that the efficiency of chlorophyll → lutein620 transfer varies significantly from monomer to monomer. Figure 6 shows the fluorescence quantum yield of LHCII as a function of E_{Lut} in which the Chl*a*612 → lutein620 channel is open in one, two, or three monomers. Obviously, decreasing the number of traps present within the trimer reduces the overall rate of fluorescence quenching. If the trimer contains only one trap, the yield at optimum E_{Lut} increases from 0.01 to 0.04.

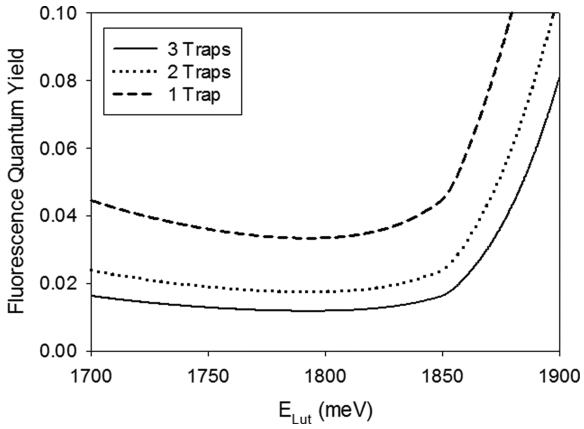

Figure 6. The fluorescence quantum yield of the LHCII trimer as a function of E_{Lut} in which the Chl*a*612 → lutein620 channel is open in one, two, or three monomers. The chlorophyll site energies are those reported by Müh et al.[53]

DISCUSSION

In the presented model, we attempted to explain the highly quenched nature of the LHCII crystal relative to the more fluorescent state observed when the trimers are in solution. By explaining this *in vitro*, aggregation-mediated quenching, we hope to shed light on the *in vivo* photoprotective qE mechanism. Recently, it has been proposed that qE occurs within LHCII, arising from the transfer of energy from the chlorophyll terminal emitter to the very short-lived, dipole-forbidden S_1 state of a closely associated lutein molecule (lutein620). By using the semiempirical MNDO-CAS-CI excited state method, we found that we could model, at least in a qualitative sense, the excited states of lutein. Unlike earlier attempts using methods like TD-DFT/TDA, this method predicted S_1 and S_2 states with the correct symmetries and oscillator strengths. This allowed for the analytical calculation of the chlorophyll−lutein620 S_1 coupling. Because of the larger distances involved, and since its S_1 state is dipole-forbidden, lutein620 has a negligible coupling to the majority of chlorophylls and only one moderately strong coupling, $J \approx 1.7$ meV (14 cm^{-1}) to the closely associated Chl*a*612. This coupling arises from the close, cofacial geometry of the two molecules.

This coupling leads to a relatively slow chlorophyll → lutein620 hopping rate ($1/k > 15$ ps) relative to the faster chlorophyll → chlorophyll kinetics ($1/k \sim 2-5$ ps for neighboring pigments). The hopping rate has a strong dependence on the relative site energies of two pigments involved (see Figure 2A). The *in situ* vertical excitation energy of lutein620 is essentially unknown, although it must be greater than ~1.72 eV (13 850 cm^{-1}), as follows from the measurements of transient and excited state absorption. The two-photon peak of lutein in solution implies a vertical energy of ~1.8 eV (14 500 cm^{-1}). The two-photon spectrum also illustrates how broad this transition is, related to the strong and rapid geometric relaxation of the S_1 state following excitation. The S_1 state is also known to have an extremely short excited state lifetime, undergoing rapid interconversion to the ground state in ~10 ps. The broadness of this transition and its short lifetime serve to make it a highly effective quencher. When LHCII is removed from the photosynthetic membrane (via detergent solubilization), it becomes highly fluorescent with an excited state lifetime of $\tau \sim 4$ ns. However, assembly into oligomers or large aggregates results in significant fluorescence quenching, reducing the excited state lifetime to $\tau \sim 0.2-1.5$ ns. The fluorescence quantum yield in the unquenched state is ~0.3, dropping to <0.04 upon aggregation. The lifetime of LHCII crystals (and therefore the atomistic structure used in our model) was measured as $\tau \approx 0.89$ ns,[44] implying a large degree of fluorescence quenching. It was observed that the presence of lutein620 in our model significantly reduced the fluorescence lifetime of the LHCII trimer. In the absence of lutein620, the excited state lifetime of the trimer is ~5 ns, resulting in a fluorescence quantum yield of ~0.3. This matches the highly fluorescent properties of chlorophyll in dilute solution. Of course, this is longer than ~4 ns due to the fact that binding of the chlorophyll to the protein results in some intrinsic (i.e., non-photoprotective) quenching. With the inclusion of lutein620 within our model, the excited state lifetime and fluorescence quantum yield decrease significantly. These quantities are very strongly dependent on E_{Lut}, not only for $E_{Lut} > E_{Chla612}$ but also for $E_{Lut} < E_{Chla612}$. Importantly, it was observed throughout that quenching by lutein620 was the most effective when $E_{Lut} \sim 1.8$ eV (14 500 cm^{-1}) was assumed (see Figures 2−4 and 6). This is somewhat lower than $E_{Chla612} \approx 1.85$ eV (14 900 cm^{-1}). However, the inherent broadness of the lutein S_1 transition ensures that chlorophyll → lutein620 hopping is highly effective even with a sizable disparity between E_{Lut} and $E_{Chla612}$, and the lower energy of the lutein620 site minimizes loss of energy back into the chlorophyll bulk. However, the model still exhibits quenching for $E_{Lut} > E_{Chla612}$, although it declines steeply with increasing E_{Lut}. At the optimum E_{Lut}, the fluorescence lifetime of the model is only ~200 ps, consistent with the strong fluorescence quenching observed in aggregated LHCII. The corresponding fluorescence yield is only ~0.01, again showing how highly quenched this structure is. We note, however, that it is more deeply quenched than the LHCII crystals. It should be noted that $E_{Lut} \approx 1.8$ eV that produced optimal quenching also coincides with the two-photon excitation peak reported by Walla et al.[61]

The role of excitonic delocalization (coherence) was tentatively studied through a simplified model, in which we assumed strong intermolecular coupling resulted in persistent delocalized states. We should note that the employed *block diagonalization* method represents a very simplified treatment of coherent effects. To correctly model the interplay between coherent coupling and dynamic localization (dephasing), a more sophisticated method, such as the hierarchical equation of motion (HEOM) approach, should be employed. Importantly, however, it was found that quenching by lutein620 was in principle identical in both the presence and absence of excitation delocalization in the terminal emmitter. Essentially, the chlorophyll−chlorophyll kinetics are irrelevant with respect to quenching, with excitations migrating to the terminal emitter in a few ps where it is effectively quenched by the closely associated lutein620. In addition to pronounced excitonic effects, we also studied the proposed role of weak excitonic delocalization across the Chla612−lutein620 dimer. It was found that this effect was too weak to produce any significant shortening of the excited state lifetime of the trimer. However, given the approximate treatment of excitonic interactions within our model and the uncertainties regarding the lutein620 site energies, we cannot exclude the possibility that significant excitonic delocalization plays a central role in the qE mechanism. Given the clear, unambiguous observation of excitonic effects by Walla et al. and other groups,[38−42] it is obvious that these effects are present to some degree within the quenched configuration of LHCII. A more formally correct treatment of coherent phenomena is needed to clarify this issue. Another limitation of our model is the neglect of the other LHCII xanthophylls (lutein, neoxanthin, and violaxanthin/zeaxanthin). This approximation was justified on the basis that we were explicitly investigating the lutein620 quenching mechanism proposed by Ruban et al.[42] Additionally, given the uncertainty regarding the xanthophyll S_1 energy, the neglect of the other xanthophylls reduced the number of free parameters in our model to one, E_{Lut620}.

In the face of these results, we must question how this model quenching mechanism reflects the fluorescence quenching inherent to LHCII crystals and, ultimately, the qE mechanism. The novelty of this work is the inclusion of chlorophyll−xanthophyll coupling, and the sophistication of the model is therefore limited by the inherent difficulty of modeling the xanthophyll S_1 state. Still we have produced xanthophyll states with the CI characters, symmetries, and optical properties. The model illustrates that lutein620 can in principle make for a highly efficient quencher if one assumes the lutein620 site energy is ∼1.8 eV, a value that agrees very well with the existing two-photon spectrum. First, is this model compatible with the observed excited state kinetics of the LHCII crystal? We see that, if we assume no heterogeneity, i.e., three identical traps per trimer, then quenching in our model is even deeper than that observed in the crystals. However, if we reduce the trap density from three to two, or even to one trap per trimer, then we obtain a quantum yield of $\varphi_F \approx 0.04$, close to the crystal value. However, this raises another important question: If this pathway reflects the true qE mechanism, then how is it switched on/off? We have observed that φ_F increases dramatically as E_{Lut} increases above ∼1.8 eV. However, some degree of quenching is always present and it is highly unlikely that E_{Lut} could be shifted by such a large degree by simple solvatochromic effects. It is more likely that some change to $J_{\mathrm{Chla612-Lut}}$ is responsible for the qE shift. This could be orientation- or distance-modulated, via small changes in the separations of the lutein620 and the chlorophyll terminal emitter. The $J_{\mathrm{Chla612-Lut}}$ implied by the crystal structure is much smaller than the typical chlorophyll−chlorophyll coupling, and it is possible that small conformational changes to the LHCII structure could reduce this already small coupling. Barzda et al.[50] and Lampoura et al.[51] have shown that such a conformational change occurs specifically within the lutein−chlorophyll domain, while the analysis of the annihilation kinetics in LHCII trimers embedded into acrylamide gel has revealed that the removing of the detergent, which mimics the native membrane environment, leads to the 3-fold increase of the quenching rate.[28] From that work, it was determined that the switch between a highly fluorescent and highly quenched state arose from internal conformational changes. Neglecting changes in the relative orientation of the pigments, it was found that changes in pigment−pigment separations of ∼10% resulted in these striking changes in spectroscopic properties. Moreover, recent time-resolved studies of single LHCII trimers have revealed these conformational states indeed exist, and LHCII trimers are constantly (although randomly) switching between them, with just the dynamic equilibrium being shifted to either one or another state, depending on the environmental conditions.[24−26] Of course, it is difficult to judge how these kinds of geometric changes would affect our model, given that we have only one atomistic structure for the complex. However, if we assume that the Chl*a*612 → lutein620 hopping rate has a Förster-type distance dependence ($1/R^6$), then an increase in separation of ∼10% (of the order of 0.5 Å) corresponds to a decrease in the hopping rate by a factor of ∼0.5. However, the true interaction between Chla612 and lutein620 is not dipole−dipole in nature, and so will have a much steeper distance dependence. Accompanied with some shift in E_{Lut}, such conformational changes probably can control the fast reversible switching to the quenching state. An extension to this model that accounts for the internal molecular dynamics of the LHCII trimer is required in order to answer this question. It is also possible that some interruption to the lutein S_1 state itself could occur either through geometric distortion or through an environmental effect such as the transient proximity of charges (possibly via protonation of a charge amino acid). Recently, the work of Wahadoszamen et al.[89] has suggested that a mixed chlorophyll−lutein620 CT state may be an important intermediate state in lutein620-mediated quenching. It is possible that such a state is very sensitive to the local charge environment and may represent the switching mechanism. This is, of course, highly speculative, and the method outlined in this paper is not appropriate for modeling such CT states. Considerable further work will be required in order to answer these questions.

One statement we can make is that the observed quenching in the LHCII crystal structure can be explained in terms of incoherent energy transfer from the chlorophyll terminal emitter to lutein620 (as suggested by Ruban et al.[42]). We found that the coupling between Chl*a*612 and lutein620 is much smaller than the most significant chlorophyll−chlorophyll couplings, implying that any excitonic mixing between the two states is likely a very minor effect. It is still possible, in principle, that weak exciton mixing can lead to a significant shortening of the excited state lifetime of the Chla612 state, although we found the Chl*a*612−lutein620 coupling too small even to induce a significant lowering of the Chl*a*612 lifetime. However, the treatment of coherence applied in this work is too simplistic

dx.doi.org/10.1021/jp3110997 | J. Phys. Chem. B 2013, 117, 10974−10986

to entirely exclude coherent interactions playing a central role in the quenching mechanism. Due to uncertainties regarding the energy of the lutein620 S_1 transition, it is also possible that significant, albeit short-lived, excitonic delocalization could occur across the chlorophyll−xanthophyll pair. We cannot therefore unambiguously exclude the possibility that such a mechanism plays a role in the qE phenomenon. A more detailed approach, such as the hierarchical equation of motion (HEOM) formalism, is needed to accurately probe the role of coherence in the chlorophyll−xanthophyll interactions. We must also note that only the direct Coulomb interaction was taken into account when we computed our transfer integrals. It is possible, particularly given the cofacial geometry of the Chl*a*612−lutein620 heterodimer, that there is some degree of π-orbital overlap, and the exchange mechanism makes an appreciable contribution to the coupling. Again, further work will be needed to address this point. Lastly, our model neglected the other xanthophylls (lutein, neoxanthin, and violaxanthin/zeaxanthin) present within LHCII. Future work will extend the theoretical framework described in this paper to the entire LHCII trimer.

CONCLUSION

We have used a combination of the TD-DFT/TDA and semiempirical MNDO-CAS-CI quantum chemistry methods to study the role of lutein in the high level of chlorophyll fluorescence of LHCII crystals. We found that the close association between lutein620 and the chlorophyll terminal emitter, coupled with the intrinsically short lifetime of the lutein620 S_1 excited state, results in significant fluorescence quenching. The kinetics of this quenching process indicates that incoherent energy transfer from Chl*a*612 to lutein620 can account for the high level of excited state quenching observed in the LHCII crystal structure. However, due to our simplified treatment of excitonic effects, we cannot exclude the possibility that coherent processes play an important role in the qE phenomenon. Importantly, we observed that the lutein620 site energy implied by existing two-photon absorption data resulted in the most effective quenching. It is possible that this mechanism is also responsible for the photoprotective qE mechanism and that nature exploits the difference in chlorophyll-*a* and lutein S1 energies to achieve highly efficient photoprotective quenching. Although this model is simple in terms of physical detail, it is the first such qE model to explicitly account for the role of xanthophylls, and we contend that it represents a fascinating new avenue of research into the qE phenomenon. Improvements to this model, such as the use of a higher level theory for the calculation of lutein excited states, a more sophisticated treatment of excitonic delocalization, the explicit inclusion of the other LHCII xanthophylls, and a more detailed description of intermolecular coupling and the solvent environment, should yield interesting results. These studies will also be coupled with the structural calculation in order to determine how the dynamics of the pigment−protein complex can regulate this mechanism.

ASSOCIATED CONTENT

Supporting Information

A description of the mathematical formalism used to compute atomic transition densities for the lutein620 S_1 transition is presented in section 1. Section 2 lists the CI composition of the lutein620 $1^1A_g^-$, $2^1A_g^-$, and $1^1B_u^+$ states. Section 3 contains several tables describing the intermolecular couplings within the trimer (S1), the calculated intermolecular hopping times (S2), the couplings between delocalized excitonic states (S3), and the calculated hopping time for transfer between delocalized excitonic states (S4). This material is available free of charge via the Internet at http://pubs.acs.org.

AUTHOR INFORMATION

Corresponding Author

Notes

The authors declare no competing financial interest.

ACKNOWLEDGMENTS

This research was supported partly by the European Social Grant under the Global Grant Measure (L.V., M.M., J.C.), UK EPSRC grant EP/H024697/1, and The Royal Society International Joint Project Grant 2009/R4. The public access supercomputer from the High Performance Computing Center (HPCC) of the Lithuanian National Center of Physical and Technology Sciences (NCPTS) at Vilnius University was used. We would like to thank Dr William Barford, Prof. James Stewart, Prof. Peter Jomo Walla, and Dr Frank Müh for their helpful advice and insight.

REFERENCES

(1) Powles, S. B. *Ann. Rev. Plant Physiol.* **1984**, *35*, 15−44.
(2) Ohad, I.; Kyle, D. J.; Arntzen, C. J. *J. Cell Biol.* **1984**, *99*, 481−485.
(3) Wraight, C.; Crofts, A. R. *Eur. J. Biochem.* **1970**, *17*, 319−327.
(4) Briantais, J. M.; Vemotte, C.; Picaud, M.; Krause, G. H. *Biochim. Biophys. Acta* **1979**, *548*, 128−138.
(5) Weis, E.; Berry, J. A. *Biochim. Biophys. Acta* **1987**, *894*, 198−208.
(6) Genty, B.; Briantais, J. M.; Baker, N. R. *Biochim. Biophys. Acta* **1989**, *990*, 87−92.
(7) Schreiber, U. *Photosynth. Res.* **1986**, *9*, 261−272.
(8) Ruban, A. V.; Johnson, M. P.; Duffy, C. D. P. *Biochim. Biophys. Acta, Bioenerg.* **2012**, *1817*, 167−181.
(9) Valkunas, L.; Trinkunas, G.; Chmeliov, J.; Ruban, A. V. *Phys. Chem. Chem. Phys.* **2009**, *11*, 7576−7584.
(10) Krause, G. H.; Behrend, U. *FEBS Lett.* **1986**, *200*, 298−302.
(11) Krause, G. H.; Laasch, H.; Weis, E. *Plant. Physiol. Biochem.* **1988**, *26*, 445−452.
(12) Noctor, G.; Rees, D.; Young, A.; Horton, P. *Biochim. Biophys. Acta* **1991**, *1057*, 320−330.
(13) Noctor, G.; Ruban, A. V.; Horton, P. *Biochim. Biophys. Acta* **1993**, *1183*, 339−344.
(14) Yamamoto, H. Y.; Kamite, L. *Biochim. Biophys. Acta* **1972**, *267*, 538−543.
(15) Yamamoto, H. Y. *Pure Appl. Chem.* **1979**, *51*, 639−648.
(16) Demmig-Adams, B. *Biochim. Biophys. Acta* **1990**, *1020*, 1−24.
(17) Li, X. P.; Björkman, O.; Shih, C.; Grossman, A. R. *Nature* **2000**, *403*, 391−395.
(18) Horton, P.; Ruban, A. V.; Wentworth, M. *Philos. Trans. R. Soc., B* **2000**, *355*, 1361−1370.
(19) Kiss, A.; Ruban, A. V.; Horton, P. *J. Biol. Chem.* **2008**, *283*, 3972−3978.
(20) Horton, p.; Ruban, A. V. *Photosynth. Res.* **1992**, *34*, 375−385.
(21) Horton, P.; Ruban, A. V.; Walters, R. G. *Annu. Rev. Plant Physiol. Plant Mol. Biol.* **1996**, *47*, 655−684.
(22) Johnson, M. P.; Goral, T. K.; Duffy, C. D. P.; Brain, A. P. R.; Mullineaux, C. W.; Ruban, A. V. *Plant Cell* **2011**, *23*, 1468−1479.
(23) Goral, T. K.; Johnson, M. P.; Duffy, C. D. P.; Brain, A. P. R.; Ruban, A. V.; Mullineaux, C. W. *Plant J.* **2012**, *69*, 289−301.
(24) Krüger, T. P. J.; Ilioaia, C.; Valkunas, L.; van Grondelle, R. *J. Phys. Chem. B* **2011**, *115*, 5083−5095.
(25) Krüger, T. P. J.; Wientjes, E.; Croce, R.; van Grondelle, R. *Proc. Nat. Acad. Sci. U.S.A.* **2011**, *108*, 13516−13521.

(26) Valkunas, L.; Chmeliov, J.; Krüger, T. P. J.; Ilioaia, C.; van Grondelle, R. *J. Phys. Chem. Lett.* **2012**, *3*, 2779−2784.
(27) Horton, P.; Ruban, A. V.; Rees, D.; Pascal, A. A.; Noctor, G. D.; Young, A. *FEBS Lett.* **1991**, *292*, 1−4.
(28) Rutkauskas, D.; Chmeliov, J.; Johnson, M. P.; Ruban, A. V.; Valkunas, L. *Chem. Phys.* **2012**, *404*, 123−128.
(29) Liu, Z.; Yan, H.; Wang, K.; Kuang, T.; Zhang, J.; Gui, L.; An, X.; Chang, W. *Nature* **2004**, *428*, 287−292.
(30) Standfuss, J.; Terwisscha van Scheltinga, A. C.; Lamborghini, M.; Kühlbrandt, W. *EMBO J.* **2005**, *24*, 919−928.
(31) Frank, H. A.; Chynwat, V.; Desamero, R. Z. B.; Farhoosh, R.; Erickson, J.; Bautista, J. *Pure Appl. Chem.* **1997**, *69*, 2117−2124.
(32) Polivka, T.; Zigmantas, D.; Sundstrom, V.; Formaggio, E.; Cinque, G.; Bassi, R. *Biochemistry* **2002**, *41*, 439−450.
(33) Holt, N. E.; Zigmantas, D.; Valkunas, L.; Li, X. P.; Niyogi, K. K.; Flemming, G. R. *Science* **2005**, *307*, 433−436.
(34) Ahn, T. K.; Avenson, T. J.; Ballottari, M.; Cheng, Y. C.; Niyogi, K. K.; Bassi, R.; Fleming, G. R. *Science* **2008**, *320*, 794−797.
(35) Ruban, A. V.; Horton, P. *Plant Physiol.* **1999**, *119*, 531−542.
(36) Ruban, A. V.; Lee, P. J.; Wentworth, M.; Young, A. J.; Horton, P. *J. Biol. Chem.* **1999**, *274*, 10458−10465.
(37) Duffy, C. D. P.; Ruban, A. V. *J. Phys. Chem. B* **2012**, *116*, 4310−4318.
(38) Liao, P. N.; Holleboom, C. P.; Wilk, L.; Kühlbrandt, W.; Walla, P. J. *J. Phys. Chem. B* **2010**, *114*, 15650−15655.
(39) Bode, S.; Quentmeier, C. C.; Liao, P. N.; Hafi, N.; Barros, T.; Wilk, L.; Bittner, F.; Walla, P. J. *Proc. Natl. Acad. Sci. U.S.A.* **2009**, *106*, 12311−12316.
(40) Liao, P. N.; Bode, S.; Wilk, L.; Hafi, N.; Walla, P. J. *Chem. Phys.* **2010**, *373*, 50−55.
(41) Mozzo, M.; Passarini, F.; Bassi, R.; van Amerongen, H.; Croce, R. *Biochim. Biophys. Acta* **2008**, *1777*, 1263−1267.
(42) Ruban, A. V.; Berera, R.; Ilioaia, C.; van Stokkum, I. H.; Kennis, J. T.; Pascal, A. A.; van Amerongen, H.; Robert, B.; Horton, P. *Nature* **2007**, *450*, 575−578.
(43) Muller, M. G.; Lambrev, P.; Reus, M.; Wientjes, E.; Croce, R.; Holzwarth, A. R. *ChemPhysChem* **2010**, *11*, 1289−1296.
(44) Pascal, A. A.; Zhenfeng, L.; Broess, K.; van Oort, B.; van Amerongen, H.; Wang, C.; Horton, P.; Robert, B.; Chang, W.; Ruban, A. V. *Nature* **2005**, *436*, 134−137.
(45) Barros, T.; Royant, A.; Standfuss, J.; Dreuw, A.; Kuhlbrandt, W. *EMBO J.* **2009**, *28*, 298−306.
(46) Ilioaia, C.; Johnson, M. P.; Horton, P.; Ruban, A. V. *J. Biol. Chem.* **2008**, *283*, 29505−29512.
(47) Kruger, T. P. J.; Ilioaia, C.; Johnson, M. P.; Ruban, A. V.; Papagiannakis, E.; Horton, P.; van Grondelle, R. *Biophys. J.* **2012**, *102*, 2669−2676.
(48) Robert, B.; Horton, P.; Pascal, A. A.; Ruban, A. V. *Trends Plant Sci.* **2004**, *9*, 387−390.
(49) Ilioaia, C.; Johnson, M. P.; Liao, P.-N.; Pascal, A. A.; van Grondelle, R.; Walla, P. J.; Ruban, A. V.; Robert, B. *J. Biol. Chem.* **2011**, *286*, 27247−27254.
(50) Barzda, V.; Peterman, E. J. G.; van Grondelle, R.; van Amerongen, H. *Biochemistry* **1998**, *37*, 546−551.
(51) Lampoura, S. S.; Barzda, V.; Owen, G. M.; Hoff, A. J.; van Amerongen, H. *Biochemistry* **2002**, *41*, 9139−9144.
(52) Novoderezhkin, V. I.; Palacios, M. A.; van Amerongen, H.; van Grondelle, R. *J. Phys. Chem. B* **2005**, *109*, 10493−10504.
(53) Müh, F.; Madjet, M. E.; Renger, T. *J. Phys. Chem. B* **2010**, *114*, 13517−13535.
(54) Müh, F.; Renger, T. *Biochim. Biophys. Acta* **2012**, *1817*, 1446−1460.
(55) Macernis, M.; Sulskus, J.; Duffy, C. D. P.; Ruban, A. V.; Valkunas, L. *J. Phys. Chem. A* **2012**, *116*, 9843−9853.
(56) Schulten, K.; Ohmine, I.; Karplus, M. *J. Chem. Phys.* **1976**, *64*, 4422−4441.
(57) Runge, E.; Gross, E. K. U. *Phys. Rev. Lett.* **1984**, *52*, 997−1000.
(58) Gross, E. K. U.; Kohn, W. *Phys. Rev. Lett.* **1985**, *55*, 2850.
(59) Kusumoto, T.; Kosumi, D.; Uragami, C.; Frank, H. A.; Birge, R. R.; Cogdell, R. J.; Hashimoto, H. *J. Phys. Chem. A* **2011**, *115*, 2110−2119.
(60) Polivka, T.; Herek, J. L.; Zigmantas, D.; Akerlund, H. E.; Sundstrom, V. *Proc. Natl. Acad. Sci. U.S.A.* **1999**, *96*, 4914−4917.
(61) Walla, P. J.; Linden, P. A.; Ohta, K.; Fleming, G. R. *J. Phys. Chem. A* **2002**, *106*, 1909−1916.
(62) Dreuw, A.; Harbach, P. H. P.; Mewes, J. M.; Wormit, M. *Theor. Chem. Acc.* **2010**, *125*, 419.
(63) Hohenberg, P.; Kohn, W. *Phys. Rev.* **1964**, *136*, 864−871.
(64) Kohn, W.; Sham, L. J. *Phys. Rev.* **1965**, *140*, 1133−1138.
(65) Yanai, T.; Tew, D. P.; Handy, N. C. *Chem. Phys. Lett.* **2004**, *393*, 51−57.
(66) Haharan, P. C.; Pople, J. A. *Theor. Chim. Acta* **1973**, *28*, 213.
(67) Frisch, M. J.; Scuseria, G. E.; Robb, M. A.; Cheeseman, J. R.; Scalmani, G.; Barone, V.; Mennucci, B.; Petersson, G. A.; Nakatsuji, H.; Caricato, M.; et al. *Gaussian 09*, revision A.1; Gaussian, Inc.: Wallingford, CT, 2009.
(68) Hirata, S.; Head-Gordon, M. *Chem. Phys. Lett.* **1999**, *314*, 291−299.
(69) Neese, F. *Wiley Interdiscip. Rev.: Comput. Mol. Sci.* **2012**, *2*, 73−78.
(70) Sherrill, C. D.; Schaefer, H. F., III. *Adv. Quantum Chem.* **1999**, *34*, 143−269.
(71) Dewar, M. J. S.; Thiel, W. *J. Am. Chem. Soc.* **1977**, *99*, 4899−4907.
(72) Stewart, J. J. P. *MOPAC2006*; 2008.
(73) Becke, A. D. *J. Chem. Phys.* **1993**, *98*, 1372−1377.
(74) Duffy, C. D. P.; Ruban, A. V.; Barford, W. *J. Phys. Chem. B* **2008**, *112*, 12508−12515.
(75) See the Supporting Information.
(76) Davydov, A. S. *Sov. Phys. Usp.* **1964**, *7*, 145.
(77) Heisenberg, W. *Z. Phys.* **1926**, *38*, 411−426.
(78) Dirac, P. A. M. *Proc. R. Soc. London, Ser. A* **1926**, *112*, 661−677.
(79) Knox, R. S.; Spring, B. Q. *Photochem. Photobiol.* **2003**, *77*, 497−501.
(80) Förster, T. *Ann. Phys.* **1948**, *437*, 55−75.
(81) Valkunas, L.; Kudzmauskas, S.; Juzeliunas, G. *Sov. Phys. Coll.* **1985**, *25*, 41−46.
(82) Zucchelli, G.; Dainese, P.; Jennings, R. C.; Breton, J.; Garlaschi, F. M.; Bassi, R. *Biochemistry* **1994**, *33*, 8982−8990.
(83) Forster, L. S.; Livingston, R. *J. Chem. Phys.* **1952**, *20*, 1315−1320.
(84) Müh, F.; Renger, T.; Zouni, A. *Plant Physiol. Biochem.* **2008**, *46*, 238−264.
(85) Yang, M.; Fleming, G. R. *J. Chem. Phys.* **2003**, *119*, 5614−5622.
(86) van Amerongen, H.; van Grondelle, R. *J. Phys. Chem. B* **2001**, *105*, 604−617.
(87) Andersso, P. O.; Gillbro, T.; Ferguson, L.; Cogdell, R. J. *Photochem. Photobiol.* **1991**, *54*, 353−360.
(88) Gradinaru, C. C.; van Stokkum, I. H. M.; Pascal, A. A.; van Grondelle, R. *J. Phys. Chem. B* **2000**, *104*, 9330−9342.
(89) Wahadoszamen, M.; Berera, R.; Ara, A. M.; Romero, E.; va Grondelle, R. *Phys. Chem. Chem. Phys.* **2012**, *14*, 759−766.